Infrared Spectroscopy and Structures of Manganese Carbonyl Cations, $Mn(CO)_n^+$ ($n = 1$–9)

Zach D. Reed and Michael A. Duncan
Department of Chemistry, University of Georgia, Athens, Georgia, USA

Manganese carbonyl cations of the form $Mn(CO)_n^+$ ($n = 1$–9) are produced in a molecular beam by laser vaporization in a pulsed nozzle source. Mass selected infrared photodissociation spectroscopy in the carbonyl stretching region is used to study these complexes and their "argon-tagged" analogues. The geometries and electronic states of these complexes are determined by comparing their infrared spectra to theoretical predictions. $Mn(CO)_6^+$ has a completed coordination sphere, consistent with its predicted 18-electron stability. It has an octahedral structure in its singlet ground state, similar to its isoelectronic analogue $Cr(CO)_6$. Charge-induced reduction in π back-bonding leads to a decreased red-shift in $Mn(CO)_6^+$ ($v_{CO} = 2106$ cm^{-1}) compared with $Cr(CO)_6$ ($v_{CO} = 2003$ cm^{-1}). The spin multiplicity of $Mn^+(CO)_n$ complexes gradually decreases with progressive ligand addition. $MnCO^+$ is observed as both a quintet and a septet, $Mn(CO)_2^+$ is observed only as a quintet, while $Mn(CO)_{3,4}^+$ are both observed as triplets. $Mn(CO)_5^+$ and $Mn(CO)_6^+$ are both singlets, as are all larger complexes. (J Am Soc Mass Spectrom 2010, 21, 739–749) © 2010 American Society for Mass Spectrometry

Transition-metal carbonyls are significant in organometallic and inorganic chemistry and provide classic examples of metal–ligand bonding [1–3]. Metal carbonyl complexes are used in synthesis and catalysis and as models for chemisorption on metal surfaces [4]. Infrared and Raman vibrational spectroscopy provides information about the structure and bonding in these systems [1–8]. In particular, the number of IR- or Raman-active vibrations and their frequencies reveals the symmetry of carbonyl complexes and their electronic structure. On surfaces, the geometrical arrangement of CO bonding can be determined from the vibrational frequency [4]. The free molecule C–O stretch occurs at 2143 cm^{-1} [9], which is well-removed from most other molecular vibrations, and provides a convenient and sensitive indicator of bonding interactions. Vibrational spectroscopy has therefore been employed to study a wide variety of metal carbonyl complexes. In the present study, we use new IR spectroscopy methods to study manganese carbonyl cations in the gas phase.

The bonding in transition-metal carbonyls is usually described with the Dewar-Chatt-Duncanson (DCD) complexation model [1, 7, 8, 10, 11]. The metal–carbonyl bond involves a synergistic interaction between a σ-type donation and π-type back-bonding. Electron density is contributed from the occupied orbitals of the carbonyl to empty orbitals on the metal, removing electron density from the partially bonding carbonyl orbitals and forming the σ bond. π-Type back-bonding stems from donation of electron density from the partially filled d-shells into the antibonding π^* orbital of the CO. In "classical" carbonyls, the C–O stretching frequency (v_{CO}) is lowered compared with its value in the free-CO molecule due to a net decrease in bonding electron density and an increase in antibonding electron density in the π^* orbitals. The majority of transition-metal carbonyl complexes exhibit a resulting red-shift in the carbonyl stretch. In rare cases, a blue-shift of this vibration is observed [12, 13]. The interplay of these σ- and π-type interactions in metal carbonyl bonding has been recognized for many years. However, recent work suggests that electrostatic interactions can provide interesting additional effects in ionized systems. Calculations suggest that metal charge may play an important role in the polarization and electron density distribution of the CO orbitals [12, 13]. Unfortunately, there are few studies of isolated gas-phase metal carbonyl ions with which to investigate these predictions.

Stable neutral transition-metal carbonyl complexes have been studied extensively in both the condensed phase and the gas-phase [6, 7, 14–19]. Neutral chromium hexacarbonyl, which is isoelectronic with manganese hexacarbonyl cation, is stable at room temperature and has been investigated spectroscopically [18, 19]. Charged transition-metal carbonyl complexes have been produced and studied in the condensed phase as salts with counterions to study isoelectronic analogues [20–23]. Various small neutral carbonyls have been studied using photoelectron spectroscopy of mass selected anions [24–26]. The electronic struc-

Address reprint requests to Dr. M. A. Duncan, Department of Chemistry, University of Georgia, 1001 Cedar St., Athens, GA 30602-2556, USA. E-mail: maduncan@uga.edu

ture and bonding in these systems cause systematic shifts in the carbonyl stretching frequency, and theory has investigated these effects extensively [7, 8, 12, 13, 27, 28].

Mass spectrometry has been used to study a number of ionic metal carbonyl complexes [29, 30]. Ion-molecule reactions have been characterized and ion-ligand dissociation energies have been measured [31–34]. Rare gas matrix isolation has been employed to study neutral, cationic, and anionic carbonyls, including those of manganese neutrals and anions [8, 35]. Gas-phase studies of carbonyl cations are limited. Free electron lasers have been used to study metal cluster ions with attached CO ligands using resonance enhanced multiphoton photodissociation [36–39]. Our research group has recently employed mass-selected infrared photodissociation spectroscopy [40, 41] to study various metal cation–carbonyl complexes in the gas phase [42–45], including $Au(CO)_n^+$ [42], $Pt(CO)_n^+$ [43], $Co(CO)_n^+$ [44], and the vanadium group systems [45]. In the present work, we use these same techniques to investigate the manganese carbonyl cation complexes $Mn(CO)_n^+$ ($n = 1–9$).

Manganese carbonyl complexes are of particular interest because of the high spin in the isolated atomic ion, which has a ^7S configuration. As CO ligands are added to this ion, ligand-electron repulsion is expected to induce spin pairing, which will gradually reduce the multiplicity, and this is expected eventually to produce a singlet state when the complete coordination is achieved. IR spectroscopy in coordination with density functional theory (DFT) studies has revealed the spin states of metal carbonyl cation systems in recent work [44, 45], and it should be possible to investigate the progression of spin changes that occur in the manganese system. The saturated binuclear complex $Mn_2(CO)_{10}$ is stable at room temperature and can dissociate into $Mn(CO)_5$ radicals [46]. Spectroscopy for both the binuclear and mononuclear neutral and anionic complexes has been reported [35j]. Photolysis of $HMn(CO)_5$ gives a $Mn(CO)_5$ radical with C_{4v} structure [46]. When the cations are considered, $Mn(CO)_6^+$ should be stable, as it satisfies the 18-electron rule and is isoelectronic to $Cr(CO)_6$. The $Mn(CO)_6^+(PF_6)^-$ salt has been isolated and ν_{CO} was measured at 2095 cm^{-1} [23]. The binding energies of $Mn(CO)_n^+$ ($n = 1–6$) in the gas phase have been determined by measuring the kinetic energy release distributions following collisional fragmentation [47]. The $MnCO^-$ ground state has been investigated by theory [48], and various manganese neutrals and anions have been studied theoretically and compared with experiment [35j]. The present study examines the infrared spectroscopy in the gas phase of both the small unsaturated $Mn^+(CO)_n$ ($n = 1–5$) complexes and larger species at or above the filled coordination ($n = 6–9$). The experimental infrared spectra are interpreted using DFT computations to probe the structure and bonding in these systems.

Experimental

$Mn(CO)_n^+$ ions are produced in a pulsed-nozzle laser vaporization source using the third harmonic of a pulsed Nd:YAG laser (355 nm; Spectra-Physics DCR-11). The laser is focused onto a rotating and translating [1/4] in. diameter manganese rod, which is mounted with a [3/4] in. horizontal offset in front of a pulsed nozzle (General Valve Series 9). The apparatus has been described in detail elsewhere [40]. The expansion gas is pure carbon monoxide (National Specialty Gases) at a backing pressure of 150 psi. Mixed clusters containing argon, i.e., $Mn^+(CO)_nAr_m$, are produced using a mixture of carbon monoxide and argon. The expansion is skimmed into a second chamber and pulse extracted into a reflectron time-of-flight mass spectrometer. Ions are mass selected using pulsed deflection plates located in the first flight tube and then excited in the turning region of the reflectron with tunable infrared light produced in an optical parametric oscillator/amplifier system (LaserVision, Bellevue, MA, USA). Pumped by the fundamental (1064 nm) of a pulsed Nd:YAG (Spectra Physics Pro 230), this system provides continuously tunable light in the region of 2000–4000 cm^{-1} with about 1 cm^{-1} line width. When cluster cations are excited on resonance with a molecular vibration, intramolecular vibrational energy relaxation (IVR) occurs on a time-scale faster than 1–2 μs (the residence time for ions in the turning region), leading to dissociation of the complex provided the binding energies are low enough. Re-acceleration out of the reflectron region disperses the fragment and parent ions in time, and spectra are obtained by monitoring the yield of a particular fragment as a function of the laser wavelength.

Density functional theory (DFT) computations were performed to investigate the structures and spin configurations of the complexes studied. Calculations for several isomers each of $Mn(CO)_n^+$ ($n = 1–7$) and $Mn(CO)_n^+$Ar ($n = 1–6$) considered the singlet, triplet, and quintet spin states. The calculations were performed using the B3LYP functional [49, 50], as implemented in the Gaussian 2003 computational package [51], using the Def 2-TZVPP basis set on all atoms [52, 53].

Results and Discussion

A mass spectrum of the $Mn(CO)_n^+$ complexes produced is shown in Figure 1, along with selected examples of infrared photofragmentation mass spectra. The most intense peak in the mass spectrum produced by the cluster source corresponds to $Mn(CO)_6^+$, indicating that this cluster cation is produced preferentially and likely has some enhanced stability. This cluster is expected to be stable as it satisfies the 18-electron rule and is isoelectronic to the well-known neutral $Cr(CO)_6$. The addition of carbonyls beyond $n = 6$ would likely result in "external" COs, that is, ligands not bound directly to the metal ion but coordinated to other carbonyls through weaker electrostatic forces. These clusters are
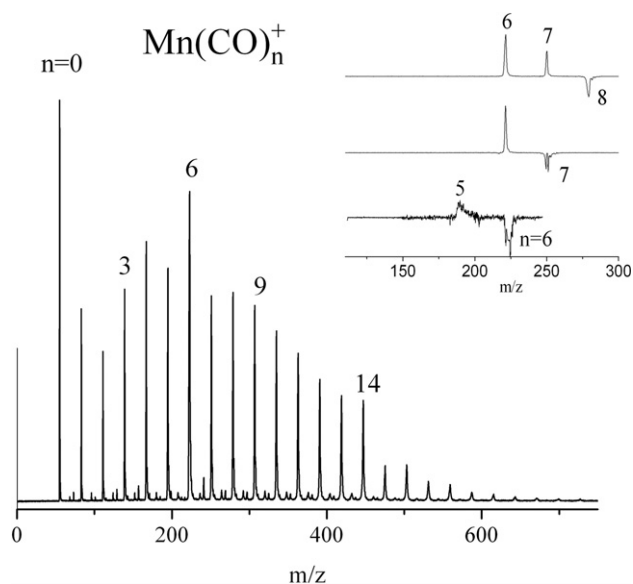
Figure 1. The mass spectrum of $Mn(CO)_n^+$ clusters produced by our cluster source. Inset: the photofragmentation mass spectra of $n = 6–8$.

produced efficiently due to the cold supersonic expansion, but are not likely to survive at room temperature.

The ligand binding energies in these complexes are investigated further by their fragmentation tendencies upon infrared excitation. Small $Mn^+(CO)_n$ clusters ($n = 1–5$) do not fragment in this experiment, consistent with the binding energies measured previously by Bowers and coworkers for these clusters, which range from 0.69 to 1.39 eV [47]. IR photons in the CO stretching region near 2100 cm^{-1} have energies of about 0.26 eV, so it is not surprising that fragmentation is not observed. The fragmentation mass spectra for $Mn(CO)_n^+$ ($n = 6–8$) are shown in the inset of Figure 1. These spectra are accumulated with a difference method by recording the mass spectrum with the fragmentation laser "on" versus "off," resulting in a negative-going parent ion (showing its depletion) and positive fragment ions. The laser was set to the wavelength that produced the maximum fragmentation yield for each parent complex. At $n = 6$, only a small amount of fragmentation is detected, and the $n = 5$ fragment ion peak shows substantial tailing in time, indicating that the excited cluster survives for a time comparable to the residence time in the reflectron ($\sim$1 μs) before dissociating. These characteristics indicate a poor fragmentation yield, consistent with the relatively high binding energy expected for this ion. The small amount of fragmentation is likely coming from multiphoton absorption or from a small fraction of ions containing residual internal energy from the growth process. At the low laser energy energies used here (about 1 mJ/pulse), we do not expect multiphoton absorption to be efficient. Residual internal energy could add to the photon energy and allow for fragmentation below the one-photon threshold. There is relatively little signal, most likely because few such hot

ions are produced. If we change conditions, we find that hotter plasmas lead to increased fragmentation, supporting the idea that internal energy contributes to the fragmentation. As shown in the figure, clusters larger than $n = 6$ fragment efficiently, and their fragmentation terminates at $n = 6$. This is consistent with the presence of weakly bound external ligands beyond this size, confirming our expectation that the six-coordinate complex is most stable.

To investigate the spectroscopy of these systems, we measure the wavelength dependence of the fragmentation. The smaller clusters do not fragment with IR excitation, so we use the "rare gas tagging" technique to study these systems [40, 41]. We produce mixed complexes of the form $Mn(CO)_n Ar_m^+$, which can fragment by eliminating argon when excited on vibrational resonances. The Mn^+-Ar binding energy has not been measured, but is calculated to be 0.131 eV (1056 cm^{-1}) [54], and should be low enough to allow fragmentation from IR excitation in the CO stretching region. As shown in Figure 2, this method allows spectra to be measured for the small ($n = 1–5$) manganese carbonyl complexes. It is of course a valid question whether or not these spectra of tagged complexes represent the desired spectra of the bare carbonyl species. Experience
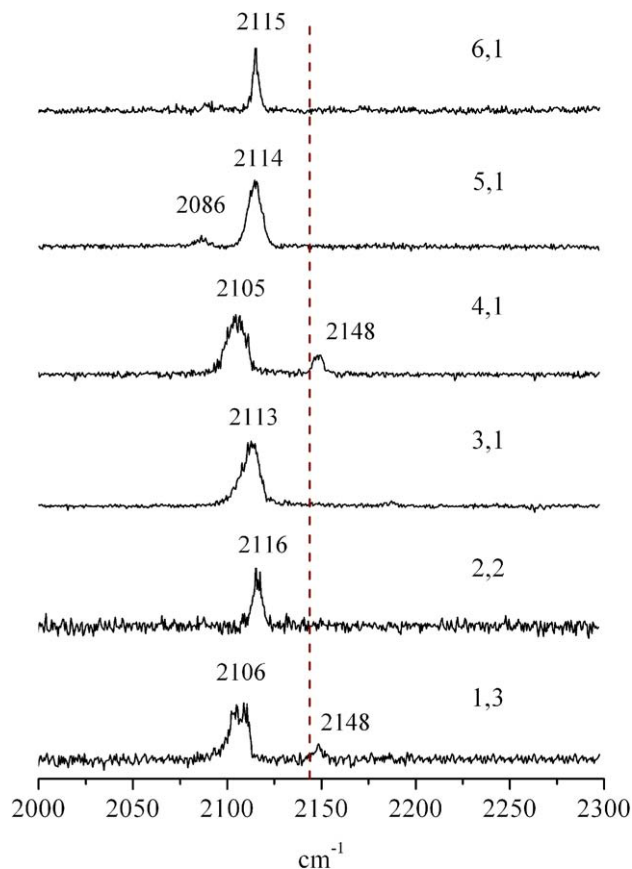

Figure 2. The infrared photodissociation spectra of small $Mn(CO)_n^+(Ar)_m$ complexes measured by the elimination of argon. The dashed vertical line shows the vibrational frequency of isolated CO in the gas phase, at 2143 cm^{-1}.

with previous systems indicates that tagging usually has a negligible effect on the structure and spectrum of the complex, but argon can bind strongly in some systems and cause a significant perturbation. With this in mind, we exercise caution in interpreting the resultant spectra and use computations on complexes with and without argon to investigate this.

Fragmentation of the $Mn(CO)^+$ complex cannot be detected when it is tagged with a single argon, presumably because the argon binding is still too strong, and even a second argon cannot be eliminated efficiently. The addition of a third argon leads to efficient fragmentation, producing the spectrum shown in the lower trace of Figure 2. In a similar way, the $Mn(CO)_2^+$ complex fragments inefficiently with a single argon, but acceptable signal is obtained with two. The $Mn(CO)_2Ar^+$ spectrum (not shown) is not significantly shifted in frequency from that of $Mn(CO)_2Ar_2^+$, indicating that the second argon is a minor perturbation on the system. All the larger complexes in the $n = 3–6$ size range fragment efficiently when tagged with a single argon. All of the spectra of these small complexes feature a strong primary band that is red shifted from the free CO frequency of 2143 cm^{-1} (indicated with the vertical dashed line in the figure), and the $n = 1, 3, 4,$ and 5 spectra contain small secondary bands. The interpretations of these spectra are discussed later, using DFT calculations to investigate the spin states, structure and spectra.

Complexes containing more than five CO ligands dissociate without tagging by the elimination of one or more CO ligands. Spectra were obtained for $n = 6$ both with and without argon, revealing the effect of tagging. The neat spectrum can be seen in the bottom trace of Figure 3 and the argon tagged spectrum is in the top trace of Figure 2. The band for the tagged complex is blue shifted by 1 cm^{-1} and is much sharper than that for the untagged species. The untagged complex would not be expected to fragment with a single photon unless it had substantial internal energy, so the broadness of the $Mn(CO)_6^+$ spectral feature is not unexpected. The tagged complex is also observed to lose CO and Ar simultaneously, and this loss channel yields a slightly different spectrum, which will be discussed later.

The spectra measured for the $n = 6–9$ complexes in the CO-loss channel are shown in Figure 3. Each features one primary band red-shifted by roughly 20 cm^{-1} from the free-CO frequency. This band does not significantly change position as more ligands are added. The increased dissociation yield after $n = 6$ and the lack of further change in the vibrational spectrum are both consistent with the presence of a six coordinate $Mn(CO)_6^+$ core ion, which becomes solvated by weakly bound external COs. A second weaker band near 2174 cm^{-1} gradually becomes prominent as additional CO ligands are added past the $n = 6$ species, and its position also does not change as more ligands are added. We assign this to the vibration of carbonyls in the second sphere, which are bound only to other
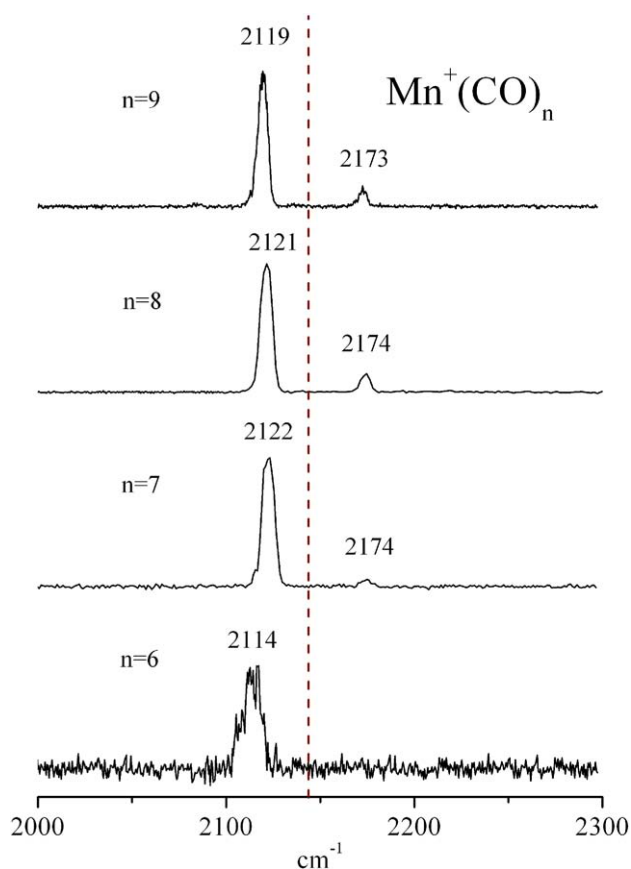

Figure 3. The infrared photodissociation spectra of larger $Mn(CO)_n^+$ complexes measured by the elimination of CO. The dashed vertical line shows the vibrational frequency of isolated CO in the gas phase, at 2143 cm^{-1}.

carbonyls and not directly to the metal ion. This behavior has been seen in other metal ion–CO complexes we have studied [43–45]. The presence of this band only after the $n = 6$ complex size again supports the conclusion of a six-coordinate $Mn(CO)_6^+$.

To gain further insight into these spectra, we have performed DFT calculations on the $Mn(CO)_n^+$ complexes for $n = 1–7$. Complete details on all the calculated structures, energetics, and spin states are provided in the Supporting Information for this paper, which can be found in the electronic version of this article. We have examined various isomers and spin states for each complex, and have also included the corresponding argon complexes at the same level of theory to investigate the effects of tagging. Table 1 summarizes the structures, electronic states, and relative energetics of the computed species. The addition of the argon causes a significant geometry perturbation in the $n = 3$ complex, but has only a minor effect on all other cluster sizes. The excellent signal levels observed in this experiment can also be understood somewhat from these theoretical results. The computed intensities of the CO stretches are generally >500 km/mol, with some in excess of 1000 km/mol (see Supporting Information). Also, second-sphere CO molecules are calcu-

Table 1. The structures, electronic ground states, and energetics computed for $Mn(CO)_n$ with DFT. No stable quintet configurations could be found for $n = 3–6$

Complex	State/structure	Relative energy (kcal/mol)
$Mn(CO)^+$	$^7C_{\infty v}$	0.0
	$^5C_{\infty v}$	+0.7
$Mn(CO)_2^+$	$^5D_{\infty h}$	0.0
	$^3D_{\infty h}$	+24.9
	$^1D_{\infty h}$	+51.6
$Mn(CO)_3^+$	$^3D_{3h}$	0.0
	$^1C_{2v}$	+9.8
$Mn(CO)_4^+$	$^1C_{2v}$	0.0
	$^3C_{3v}$	+8.8
$Mn(CO)_5^+$	$^1C_{4v}$	0.0
	$^3D_{3h}$	+8.7
$Mn(CO)_6^+$	^1O_h	0.0
	$^3C_{4h}$	48.0

lated to be bound by about 600 cm^{-1}. Although the van der Waals binding in this situation is not expected to be handled particularly well by DFT, the weak binding suggested is low enough to allow for efficient photodissociation for the larger complexes.

We find that $Mn^+(CO)$ is linear for all spin states, and DFT predicts a septet ground state, although this is favored by only 0.75 kcal/mol over the quintet. The triplet lies another 33 kcal/mol higher in energy from the quintet. For the bare cation, the ^7S state is 9472.97 cm^{-1} (27 kcal/mol) lower in energy than the ^5S state [55]. The addition of a single argon only minimally perturbs the geometry of the $Mn^+(CO)$ system and results in an overall linear structure. Addition of a second argon leads to a small distortion producing a C_{2v} structure. The $Mn^+(CO)_2$ complex has a linear quintet ground state, with higher energy triplet and singlet states. The argon binds on the side of this, producing a slightly bent C_{2v} structure. $Mn^+(CO)_3$ has a triplet D_{3h} structure, with a C_{2v} singlet species lying 10 kcal/mol higher in energy. The triplet is deformed

significantly by the addition of argon, into a structure resembling that of the singlet. For $Mn^+(CO)_4$, a C_{2v} singlet structure is predicted to be more stable than a triplet C_{3v} species by about 9 kcal/mol. The singlet is only slightly perturbed by the addition of argon, while the triplet again distorts towards the singlet geometry. The singlet-triplet energy difference is nearly the same for $Mn^+(CO)_5$, and again the singlet is predicted to be more stable with a C_{4v} structure. The distortion caused by argon is again small for this complex. $Mn^+(CO)_6$ is predicted to be an octahedral singlet, some 48 kcal more stable than the triplet configuration. This complex is also virtually unchanged by the addition of argon. No minimum structure could be found for a seven-coordinate $Mn(CO)_7^+$ complex; all starting geometries converged to structures with a central octahedral core and an external CO ligand capping the octahedron. This is consistent with the previous conclusion that six carbonyl molecules complete the coordination sphere around Mn^+.

The influence of argon tagging on the spin states of these clusters is worth mentioning. We have studied this most extensively for the smaller clusters ($n = 1–3$), where tagging with multiple argons is required to detect photodissociation. In these systems, one would expect that added argon, which binds rather strongly, would preferentially stabilize lower spin states in much the same way that added CO molecules do, but to a lesser degree. However, we do not at all find this to be the case. As shown in the computed energetics provided in the Supporting Information, the septet state in these small clusters retains its relative stability compared with the quintet state upon the addition of argon, and in some cases it actually gains stability by a small amount. This behavior is surprising, but it gives us more confidence that our tagged systems are representative of the corresponding untagged species.

Table 2 gives a comparison between the computed and measured frequencies for the neat and argon

Table 2. The vibrational frequencies computed (scaled by 0.9679) and measured for $Mn(CO)_n^+$ and $Mn(CO)_n(Ar)_m^+$ complexes

Complex	Theory (neat)	Theory (argon-tagged)	Experiment
$Mn(CO)^+$			
Septet	2210.1	2158.2 (m = 1), 2141.5 (m = 2)	2106, 2148
Quintet	2132.8	2122.3 (m = 1), 2106.4 (m = 2)	
$Mn(CO)_2^+$			
Quintet	2127.4	2114.6	2116
$Mn(CO)_3^+$			
Triplet	2146.1	2091.1, 2130.3, 2170.1	2113, 2187
$Mn(CO)_4^+$			
Triplet	2077.0, 2150.1, 2150.4 2123.1	2072.6, 2138.6, 2138.7, 2172.8 2167.4	2105, 2148
Singlet	2097.7, 2109.3 2123.1	2086.8, 2103.6 2167.4	
$Mn(CO)_5^+$			
Singlet	2099.9, 2119.3	2097.0, 2114.2	2086, 2114
Triplet	2148.7	2095.9, 2148.3	
$Mn(CO)_6^+$			
Singlet	2118.4	2119.4	2115
Triplet	2074.1, 2158.2	2073.7, 2158.7	

tagged complexes. The calculated frequencies are scaled by 0.9679 and given a 3 cm^{-1} FWHM Lorentzian line shape to produce computed spectra to compare to the experimental data. The scaling factor was chosen to make the calculated CO stretching frequency match the experimental free molecule value. Figure 4 shows the computed and experimental spectra for the $n = 1$–2 complexes, along with their computed ground state geometries. In the case of the $n = 1$ complex, a spectrum with good signal level could only be measured when three argon atoms were attached, but the computations failed to converge for this 1,3 species. However, a very noisy spectrum of the $n = 2$ species has the large band in essentially the same position as that in the $n = 3$ spectrum. Therefore we assume that the third argon does not introduce a significant additional perturbation compared with the second and we present the computational results for the two spin states of the 1,2 species to compare to the spectrum measured for the 1,3 species. Mn$^+$(CO)Ar$_3$ has two experimental IR bands, but theory for each of the two likely spin states of Mn$^+$(CO)Ar$_2$ predicts only a single band. This of course makes sense because there is only one CO group present in the complex. The two experimental bands then suggest that there is more than one isomeric structure or spin state present. The septet and quintet configurations spin configurations have nearly the
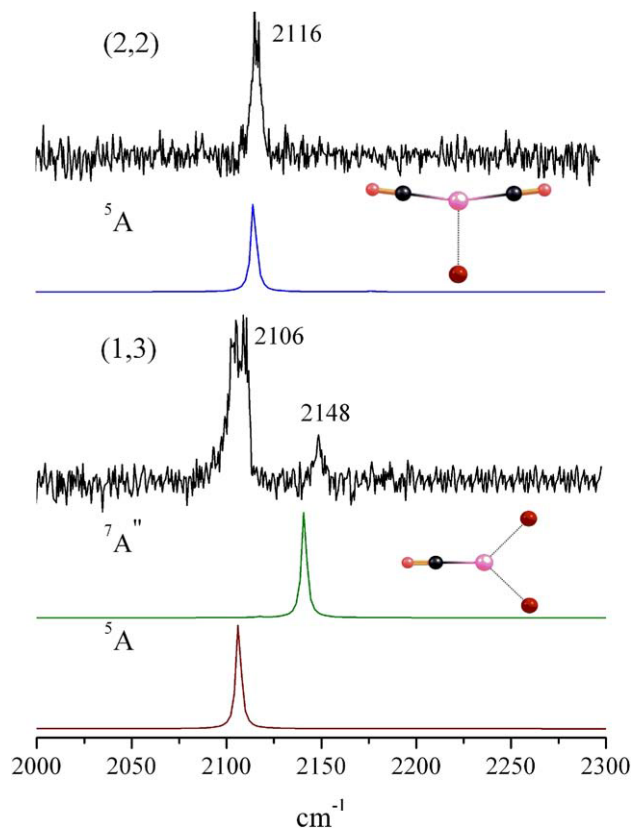

Figure 4. Infrared spectra of Mn(CO)$_n$Ar$_m^+$ ($n = 1$, 2) compared with the spectra predicted by theory, along with calculated ground state structures.

same computed energies, with the triplet lying some 33 kcal/mol higher. As shown in Table 2, the addition of one or two argons to the Mn(CO)$^+$ species causes significant vibrational band shifts and so it is essential to compare our spectra to those predicted for the argon tagged species. When we do this, the septet spin complex has a predicted band at 2141.5 cm^{-1} and the quintet has its band at 2114 cm^{-1}, which compare favorably with the bands measured at 2148 and 2106 cm^{-1}. The computed oscillator strengths for these bands are nearly identical at 544 km/mol, so the observed intensities should reflect roughly the relative populations. We therefore conclude that both the septet and quintet spin states are present, with a greater population for the quintet.

In the $n = 2$ complex, we could only measure the spectrum with good signal level when the complex was tagged with two argons. The resulting 2,2 spectrum is shown in the upper trace of Figure 4. Again in this system, we could not get the computational studies to converge for the desired 2,2 complex, and so we present the data for the 2,1 species. We were able to measure a very noisy spectrum for the 2,1 species (not shown) and its band position was the same as that for the 2,2 species, validating this comparison. The computed structure for the 2,1 complex is slightly bent, with argon bound to the metal ion on the side of the OC-Mn$^+$-CO axis. The quintet spin configuration lies 25 kcal/mol lower than the corresponding triplet. The calculated frequency for the bent quintet is 2115 cm^{-1}, which matches our experimental band position of 2116 cm^{-1}, whereas the triplet state frequency is calculated to be 2096 cm^{-1}. Because of the large computed energy difference between the spin states and the excellent spectral agreement, we assign this complex as a quintet.

The experimental and calculated spectra and structures for the $n = 3,4$ complexes are presented in Figure 5. In these systems we measured the spectra with single-argon tagging and were also able to complete the computations on these same species. For $n = 3$, the neat complex is computed to have a D$_{3h}$ structure, while the argon-tagged species distorts to a C$_{2v}$ configuration, which is shown in Figure 5. The triplet state is computed to be around 10 kcal/mol more stable than the singlet species. Its predicted spectrum agrees reasonably well with the experiment, matching the positions of the most intense band at 2113 cm^{-1} and that of a weak band at 2187 cm^{-1}, but a small band predicted at 2135 cm^{-1} is not detected in our spectrum. The singlet structure is only minimally perturbed by the addition of argon, and it has a predicted spectrum with a doublet of bands at 2096/2116 cm^{-1}. We do not detect a doublet, but our peak assigned at 2113 cm^{-1} is wide enough so that an unresolved doublet could conceivably be present. The singlet spectrum also predicts a single small band at 2168 cm^{-1}, which is not a particularly good match for the experimental band at 2187 cm^{-1}. From this comparison, apparently the best match to the spectrum is found for the triplet spin state, which is
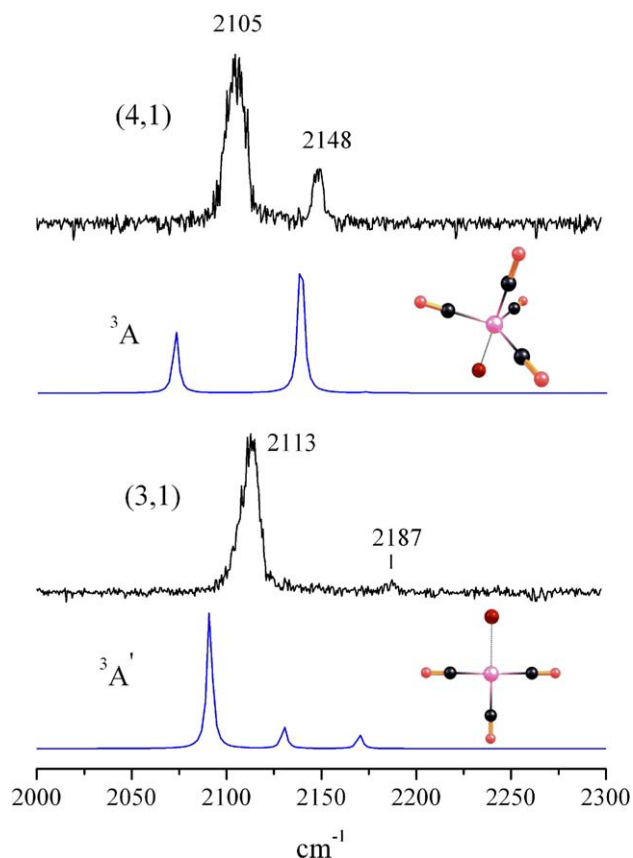
Figure 5. Infrared spectra of $Mn(CO)_nAr_m^+$ ($n = 3, 4$) compared with the spectra predicted by theory, along with calculated ground state structures.

computed to be most stable. However, we cannot completely rule out the singlet spin state.

For the $n = 4$ species, the computed structure has a C_{2v} symmetry for both the neat and the tagged complex in each of the triplet and singlet spin states. The singlet is predicted to be more stable than the triplet by 8.8 kcal/mol. However, the spectrum predicted for the singlet does not match the experimental pattern. It has two main bands at 2086 and 2104 cm^{-1} with roughly equal intensity, with sufficient separation that we should be able to resolve them if they were present, and another much weaker band at 2167 cm^{-1}. This pattern does not match either the spacing or the relative intensities of the experimental bands. On the other hand, the predicted triplet complex has two main bands whose positions are red shifted somewhat from those in the spectrum, but whose spacing nearly matches that measured. The intensity ratio, however, is reversed between the theory and experiment. When the triplet state calculation was repeated with a different basis set, e.g., 6-31+G* on C, O, and Ar and LANL2DZ on Mn, the predicted neat spectrum was nearly identical to that calculated with the TZVPP basis. However, the argon-tagged spectrum preserved the band spacing but swapped band intensity ratios, matching the experiment better. It thus appears that the magnitude of the

perturbation caused by the argon is quite sensitive to the basis set employed, and indeed it may not be well described with the TZVPP basis. This particular cluster size is therefore problematic, but apparently the higher energy triplet spin state agrees with the experiment better than the singlet. If we assume that $n = 4$ is in fact a triplet, then likely the $n = 3$ complex is also a triplet, consistent with our earlier conclusion. It seems unlikely that a smaller complex would have a lower spin, since ligand-electron repulsion is the mechanism causing the progressive spin pairing.

Figure 6 shows the experimental and calculated spectra for the $n = 5$ and 6 complexes, along with their ground state geometries. The $n = 5$ complex has a C_{4v} square pyramid structure for the singlet spin state and a slightly distorted trigonal bipyramid structure for the triplet state. Neither the singlet or triplet configuration is deformed significantly by the addition of argon. Here the singlet is predicted to be more stable by 8.8 kcal/mol. It has two bands, at 2097 and 2114 cm^{-1}, whose positions and intensity ratio matches quite nicely with our observed spectrum. The triplet is predicted to have a 2096 cm^{-1} band, and a doublet split by 0.5 cm^{-1} at 2148 cm^{-1}, which we do not observe. We can therefore
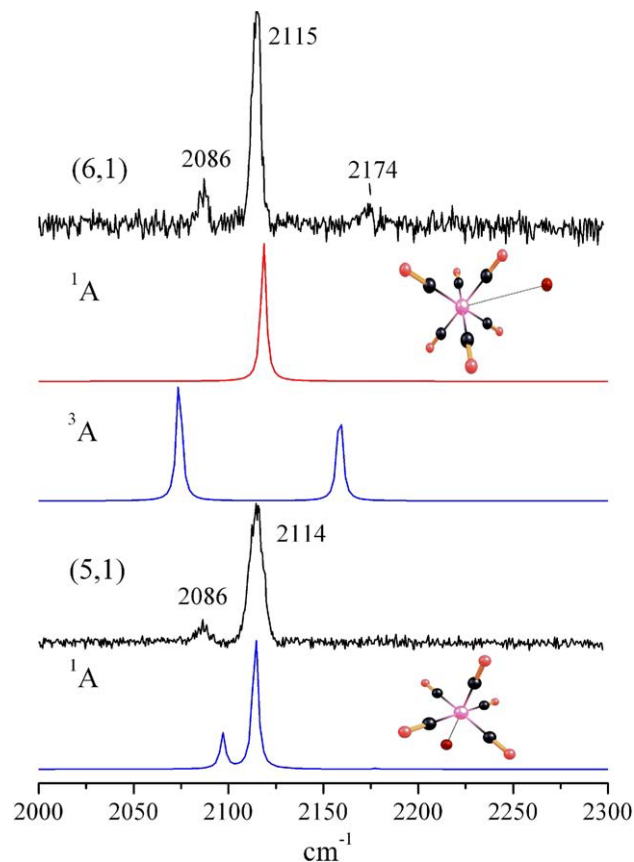

Figure 6. Infrared spectra of $Mn(CO)_nAr_m^+$ ($n = 5, 6$) compared with the spectra predicted by theory, along with calculated ground state structures. The $Mn(CO)_6Ar^+$ spectra was measured by loss of Ar + CO, the $Mn(CO)_5Ar^+$ spectra was measured by loss of CO.

exclude the triplet and conclude that the $n = 5$ complex has a singlet ground state and the C_{4v} structure.

The $n = 6$ complex is computed to have the expected octahedral structure and a singlet ground state, which is predicted to be 48.0 kcal/mol more stable than the triplet. The triplet has a slightly distorted D_{4h} structure in which one pair of axial bonds is slightly lengthened relative to the octahedron. The addition of argon to the singlet species has a negligible effect on the vibrational spectrum; we were unable to get the argon complex for the triplet to converge. Experimentally, we are able to obtain spectra for both the neat and Ar tagged versions of this complex. Figure 6 shows the Ar tagged spectrum, measured by the loss of Ar and CO, while the spectrum of this same complex in the more intense argon-loss channel is in the top trace of Figure 2. The neat spectrum measured by loss of CO can be found in the bottom pane of Figure 3. The main band position is virtually identical in these three spectra (2114, 2115, and 2115 cm^{-1}, respectively), differing only in the increased line width in the CO-loss spectrum. The spectrum in Figure 6 measured by tagging (Ar and CO elimination) has a slight trace of two additional bands, one at 2086 and another at 2174 cm^{-1}. The spectrum measured in the loss of argon only has a better signal level but shows only the single main band at 2115 cm^{-1}. As shown in Figure 6, the spectrum computed for the O_h singlet configuration matches the position of the single main band perfectly, confirming that this is the structure and ground state for this complex. This is consistent with previous work, in which the Mn(CO)$_6^+$ ground state was determined to be a singlet by various methods [53, 56, 57]. The weak features in the Mn(CO)$_6^+$ spectrum in Figure 6 were found to increase in intensity when the laser plasma was hotter, and these bands could be eliminated entirely under our coldest conditions. The next-lowest excited-state is the triplet, and so we present its computed spectrum as the blue trace in the middle of the figure. Because the tagged triplet species did not converge, we present the spectrum here computed for the untagged complex. Although the experimental intensity is quite small, it is evident that the spectrum for the triplet species matches these two bands quite well in position and intensity ratio. If these bands are indeed from the triplet state, this would mean that a small amount of this much higher energy species can be produced under hot plasma conditions and that this metastable state can survive the addition of argon and the transit through the apparatus, which takes several hundred microseconds. Another assignment possible for the weaker bands here, and perhaps more plausible, is that they represent another isomer with five COs coordinated to the metal and one external. As shown in the lower part of Figure 6, the $n = 5$ species has a main band at 2114 cm^{-1}, which would overlap that of the $n = 6$ species, and also a weak band at 2086 cm^{-1} in the same place as that for the weak $n = 6$ band. The other weak band for the $n = 6$ species at 2174 cm^{-1} is quite close to the position for second-shell CO. From

the information available, the minor bands for $n = 6$ under hot conditions could therefore come from either a small amount of the five-coordinate isomer or the triplet spin state.

The Mn(CO)$_6^+$ species identified here can be compared with its counterpart ion, which has been isolated as a salt with a counterion present [23]. The CO stretching frequency of 2095 cm^{-1} [23] for the condensed phase [Mn(CO)$_6^+$][PF$_6^-$] salt varies by some 20 cm^{-1} from the value of 2115 cm^{-1} seen here in the gas phase. The effect of the condensed phase environment is small, but non-negligible. The vibrational frequency for Mn(CO)$_6^+$ can also be compared with the value for its isoelectronic analogue Cr(CO)$_6$, whose CO stretch occurs at 2003 cm^{-1} [19]. As shown here, the manganese cation complex has the same structure and ground state as the neutral chromium complex, but the neutral species has a CO stretch that is red-shifted by more than 100 cm^{-1} compared with the value for the cation. This large difference between ion complexes and their isoelectronic neutral analogues has also been seen in other systems, as we have discussed in a recent paper from our group on the Co(CO)$_5^+$ species, which is isoelectronic to Fe(CO)$_5$ [44]. Table 3 summarizes a comparison between the corresponding neutral and ionic complexes, presenting the results of experimental and computational work on the present system as well as that of the Co$^+$/Fe systems. The Co(CO)$_5^+$ and the Fe(CO)$_5$ complexes both have trigonal bipyramid structures with singlet ground states. Co(CO)$_5^+$ has two carbonyl stretches at 2140 and 2150 cm^{-1} [44], while Fe(CO)$_5$ has these same vibrations at 2013 and 2034 cm^{-1} [15]. Like the Mn$^+$/Cr comparison in the present work, the ionized cobalt complex has a much smaller red shift in its vibrations than the isoelectronic iron neutral. As noted earlier, the nature of charge-transfer between the CO ligand and the metal are well known to be the source of the red shift in the CO stretch compared with its gas-phase value in isolated CO. σ-Donation should be enhanced in cation systems relative to their neutrals, as the cation charge should draw electron density toward it. If this were the most important factor, then cation species should have greater red shifts in their vibrations than corresponding neutrals, opposite to the observed trend. On the other hand, π back-

Table 3. Comparison of experimental frequencies to calculated frequencies and oscillator strengths of the isoelectronic analogues Mn(CO)$_6^+$, Cr(CO)$_6^+$, and Co(CO)$_5^+$, Fe(CO)$_5$

Species	Experimental frequency	Calculated frequency	Oscillator strength
Mn(CO)$_6^+$	2115	2118.5	1061
Cr(CO)$_6$	2002.9[a]	2001.2	1861
Co(CO)$_5^+$	2140, 2150[b]	2140.0, 2154.1	644, 761
Fe(CO)$_5$	2013, 2034[c]	2008, 2036	1268, 1456

[a]Reference [19].
[b]Reference [44].
[c]Reference [15].

bonding interactions should be less effective in cations than neutrals because of the tendency of the cations to retain their electrons. If this is more important, then neutrals should have more red-shifted vibrations than cations, consistent with the trends shown in the table. These studies therefore confirm the primary importance of π back-bonding in these carbonyl vibrational shifts, which has indeed been pointed out in many previous studies [1, 2, 6–8]. In another example of this effect, the isoelectronic series of $Ni(CO)_4$, $Co(CO)_4^-$, and $Fe(CO)_4^{2-}$ were studied previously, which have CO stretching frequencies of 2094, 1946, and 1799 cm^{-1} respectively [15, 20, 22]. Here the neutral has inefficient back-bonding, while this increases with charge for anions. The results suggested here in our cation studies are therefore completely consistent with the previous understanding of the shifts for carbonyl stretches in metal complexes.

The data in Table 3 also allow a comparison of the computed IR intensities of the CO vibrations for neutrals versus ions. Comparing the isoelectronic pairs of $Mn(CO)_6^+/Cr(CO)_6$ and $Co(CO)_5^+/Fe(CO)_5$, we find in both cases that the neutrals have more intense vibrations than the cations. The neutral oscillator strengths are in fact nearly a factor of two greater than those of the ions. This trend is somewhat surprising, because vibrational motion next to a charge often enhances the IR oscillator strength. For example, we have recently found much stronger O–H stretches in cation–water complexes than in the free water molecule, and the doubly charged complexes were found to have much stronger transitions than those of the singly charged complexes [56]. Apparently, the trend for carbonyl ligands is reversed, at least in these two examples. This is perhaps related to subtle effects of the charge distribution on the CO induced by metal bonding, which have been discussed previously [13].

With the octahedral ion identified here as the stable species in this system, we can consider the effects of adding more CO ligands to this system. We expect that additional ligands beyond this stable coordination will be added in the form of weakly bonded external species. However, as we have recently shown for niobium and tantalum carbonyls [45], higher coordination is sometimes possible. Figure 3 shows the spectra that we have measured for the larger complexes. They exhibit higher dissociation yields, consistent with the presence of weakly bound ligands, and their spectra each have one main vibrational band now recognized to be very close to the position of the single feature expected for the octahedral complex. To investigate this further, we have performed a computational study on the $n = 7$ complex. The spectra and calculated structure are found in the Supporting Information. No stable seven-coordinate complex could be found, and the $n = 7$ species invariably converged to a six-coordinate core with one external CO ligand. The agreement between the theoretical calculation and experiment is excellent. The main vibrational band is predicted to shift slightly to the blue

(2119 cm^{-1}) compared with its position in the $n = 6$ complex, consistent with the experiment. In the experiment, the main v_{CO} stretch moves slightly as additional CO ligands are added, reaching 2119 cm^{-1} by the third external CO at the $n = 9$ complex. Additionally, the weak intensity blue-shifted band associated with the external or second-sphere CO molecules is also reproduced. The external CO band is observed to shift slightly to the red, from 2175 cm^{-1} for the $n = 7$ complex to 2172 cm^{-1} for the $n = 9$ complex, also gaining intensity as more external COs are present. These frequencies are some 30 cm^{-1} to the blue from the free CO stretch at 2143 cm^{-1}. The computed position of this band for the $n = 7$ complex is 2133 cm^{-1}, which is significantly higher in frequency than the main vibrational band of the core $Mn(CO)_6^+$ ion, but still not nearly as far to the blue as it is observed in the experiment (2174 cm^{-1}). This is consistent with the behavior that we have found previously for this kind of external-CO vibration in the analogous $Co(CO)_n^+$ complexes [44]. As we discussed in that work, Goldman and Krogh-Jespersen [12] have proposed that slight polarization of such an external CO near a charged system could cause a blue shift in the C–O frequency, in a way analogous to how this shift occurs for so-called "non-classical" metal carbonyls with closed-shell metal ions [12, 13, 42, 43]. This concept explains how a shift to higher frequency can occur, but the magnitude of this effect is apparently not reproduced by the present level of theory.

Conclusion

Manganese carbonyl cations of the form $Mn(CO)_n^+$ ($n = 1–9$) and their corresponding "argon-tagged" analogues $Mn(CO)_n(Ar)_m^{2+}$ were produced and studied using mass selected infrared photodissociation spectroscopy and density functional theory. Comparison of the number of infrared bands, along with their positions and intensities, allows us to assign the electronic configuration and geometry for these complexes. A gradual spin change is observed as sequential carbonyl ligands are added. The $MnCO^+$ complex has both quintet and septet population, with a quintet ground state. $Mn^+(CO)_2$ also has a quintet ground state, while $Mn(CO)_{3-4}^+$ complexes are triplets. The $Mn(CO)_5^+$ and $Mn(CO)_6^+$ complexes are both singlets. $Mn(CO)_6^+$ has a completed coordination shell, in line with its expected 18 electron stability, and shares an octahedral structure with its isoelectronic analogue, $Cr(CO)_6$. The carbonyl stretches for $Mn(CO)_6^+$ are *less* red-shifted than those in $Cr(CO)_6$, due to the reduced π back-bonding caused by the charge. However, the oscillator strengths of the neutral analogues are *greater* than those the cations.

Density functional theory provides significant insight into the structures and spectra of these ions. For the most part, it provides what appears to be an accurate portrayal of these systems. One problem case is the $Mn(CO)_4^+$ complex, which is predicted to have a singlet ground state but found to have a triplet. The

potential problems with DFT for studies of transition-metal complexes and their spin states are well known [57], and so some issues of this type are not at all unexpected. Likewise, DFT is known to have difficulties with weak bonding interactions such as those in van der Waals systems. In the present case, the effects of argon binding are handled well for the most part. This is likely because the argon binding energies in the small complexes are actually quite substantial. However, the vibrational frequencies of the external COs solvating the core $Mn(CO)_6^+$ ion are not handled quantitatively, and this is then understandable.

These infrared spectroscopy studies on mass-selected ions compare favorably, where comparisons are possible, with results from traditional inorganic chemistry in the condensed phase. However, our studies allow the effects of solvents and counterions to be removed, thus providing a more direct comparison to the results of theory. Additionally, these studies allow the systematic investigation of properties for the coordinatively unsaturated species, which cannot be studied in traditional chemistry. In the present system, this allows the progressive changes in spin states as CO ligands are added to the Mn^+ ion to be observed for the first time.

The Supporting Information contains the full details of the DFT computations done in support of the spectroscopy here, including the structures, energetics, and vibrational frequencies for each of the structures considered. The complete reference for Reference [51] is also included in the Supporting Information.

Acknowledgments

Appendix A
Supplementary Material

Supplementary material associated with this article may be found in the online version at doi:10.1016/j.jasms.2010.01.022.

References

1. Cotton, F. A. *Advanced Inorganic Chemistry*, 6th ed.; John Wiley and Sons, Inc.: New York, 1999.
2. Huheey, J. E.; Keiter, E. A.; Keiter, R. L. *Inorganic Chemistry Principles of Structure and Reactivity*; Harper Collins: New York, 1993.
3. Wrighton, M. The Photochemistry of Metal Carbonyls. *Chem. Rev.* **1974,** *74,* 401.
4. Somorjai, G. A. *Introduction to Surface Chemistry and Catalysis*; John Wiley and Sons, Inc.: New York, 1994.
5. Bertini, I.; Gray, H. B.; Stiefel, E. I.; Valentine, J. S. *Biological Inorganic Chemistry Structure and Reactivity*; University Science Books: Sausalito, CA, 2007.
6. Nakamoto, K. *Infrared and Raman Spectra of Inorganic and Coordination Compounds*; John Wiley: New York, 1997.
7. Frenking, G.; Fröhlich, N. The Nature of the Bonding in Transition-Metal Compounds. *Chem. Rev.* **2000,** *100,* 717.
8. Zhou, M.; Andrews, L.; Bauschlicher, C. W. Spectroscopic and Theoretical Investigations of Vibrational Frequencies in Binary Unsaturated Transition-Metal Carbonyl Cations, Neutrals, and Anions. *Chem. Rev.* **2001,** *101,* 1931.
9. Huber, K. P.; Herzberg, G. *Molecular Spectra and Molecular Structure IV. Constants of Diatomic Molecules*; Van Nostrand Reinhold Co.: New York, 1979, p. 166.
10. Chatt, J.; Duncanson, L. A. Olefin Coordination Compounds. III. Infrared Spectra and Structure: Attempted Preparation of Acetylene Compounds. *J. Chem. Soc.* **1953,** 2939.
11. Dewar, M. J. S. S. A Review of the π-Complex Theory. *Bull. Soc. Chim. Fr.* **1951,** *18,* C79.
12. Goldman, A. S.; Krogh-Jespersen, K. Why Do Cationic Carbon Monoxide Complexes Have High CO Stretching Force Constants and Short CO Bonds? Electrostatic Effects, Not σ Bonding. *J. Am. Chem. Soc.* **1996,** *118,* 12159.
13. (a) Lupinetti, A. J.; Frenking, G.; Strauss, S. H. Nonclassical Metal Carbonyls. *Angew. Chem. Int. Ed.* **1998,** *37,* 2113. (b) Lupinetti, A. J.; Jonas, V.; Thiel, W.; Strauss, S. H.; Frenking, G. Trends in Molecular Geometries and Bond Strengths of the Homoleptic d10 Metal Carbonyl Cations: A Theoretical Study. *Chem. Eur. J.* **1999,** *5,* 2573. (c) Lupinetti, A. J.; Fau, S.; Frenking, G.; Strauss, S. H. Theoretical Analysis of the Bonding between CO and Positively Charged Atoms. *J. Phys. Chem.* **1997,** *101,* 9551.
14. O'Dwyer, M. F. Infrared Spectra and Normal Coordinate Analysis of Iron Pentacarbonyl. *J. Mol. Spectrosc.* **1958,** *2,* 144.
15. Jones, L. H.; McDowell, R. S.; Goldblatt, M. Potential Constants of Iron Pentacarbonyl from Vibrational Spectra of Isotopic Species. *J. Chem. Phys.* **1972,** *57,* 2050.
16. Boquet, G.; Birgone, M. Infrared Spectra of Ni(CO)4 in Gas Phase. *Spectrochim. Acta* **1971,** *27,* 139.
17. Beagley, B.; Schmidling, D. G. A Re-evaluation of the Molecular Structure of Iron Pentacarbonyl. *J. Mol. Struct.* **1974,** *22,* 5466.
18. Shufler, S. L.; Sternberg, H. W.; Friedel, R. A. Infrared Spectrum and Structure of Chromium Hexacarbonyl, $Cr(CO)_6$. *J. Am. Chem. Soc.* **1956,** *78,* 2687.
19. Hansford, G. M.; Davies, P. B. Infrared Laser Spectroscopy of Jet-Cooled Chromium Hexacarbonyl in the 5 μ Region. *J. Mol. Spec.* **1994,** *168,* 540.
20. Stammerich, H.; Kawai, K.; Tavares, Y.; Krumholz, P.; Behmoiras, J.; Bril, S. Infrared Spectra of $Fe(CO)_4^{2-}$ in Aqueous Solution. *J. Chem. Phys.* **1960,** *32,* 1482.
21. Abel, E. W.; McLean, A. N.; Tyfield, S. P.; Braterman, P. S.; Walker, A. P.; Hendra, P. J. Infrared Spectra of $V(CO)_6^-$ and $Re(CO)_6^+$ in CH_3CN solution. *J. Mol. Spectrosc.* **1969,** *30,* 29.
22. Edgell, W. F.; Lyford, J. I. Infrared Spectra of $Co(CO)_4^-$ in DMF Solution. *J. Chem. Phys.* **1970,** *52,* 4329.
23. McLean, R. A. N. Infrared and Raman Spectra of $Mn(CO)_6^+$ in CH_3CN Solutions and Solids. *Can. J. Chem.* **1974,** *52,* 213.
24. Engelking, P. C.; Lineberger, W. C. Laser Photoelectron Spectrometry of the Negative Ions of Iron and Iron Carbonyls. Electron Affinity Determination for the Series $Fe(CO)_n$, $n = 0, 1, 2, 3, 4$. *J. Am. Chem. Soc.* **1979,** *101,* 5579.
25. (a) Villalta, P. W.; Leopold, D. G. A Study of the FeCO and the s and s States of FeCO by Negative Ion Photoelectron Spectroscopy. *J. Chem. Phys.* **1993,** *98,* 7730. (b) Bengali, A. A.; Casey, S. M.; Cheng, C. L.; Dick, J. P.; Fenn, P. T.; Villalta, P. W.; Leopold, D. G. Negative Ion Photoelectron Spectroscopy of the Coordinatively Unsaturated Group VI Metal Carbonyls of Chromium, Molybdenum, and Tungsten. *J. Am. Chem. Soc.* **1992,** *114,* 5257.
26. Butcher, C. P.; Johnson, B. F. G.; McIndoe, J. S.; Yang, X.; Wang, X. B.; Wang, L. S. Collision-Induced Dissociation and Photodetachment of Singly and Doubly Charged Anionic Polynuclear Transition Metal Carbonyl Clusters $Ru_3CO(CO)_{13}^-$, $Ru_6CO(CO)_{16}^{2-}$ $Ru_6CO(CO)_{18}^{2-}$. *J. Chem. Phys.* **2002,** *116,* 6560.
27. Barnes, L. A.; Rosi, M.; Bauschlicher, C. W. Theoretical Studies of the First- and Second-Row Mono- and Dicarbonyl Positive Ions. *J. Chem. Phys.* **1990,** *93,* 609.
28. Huo, C.-H.; Li, Y.-W.; Wu, G.-S.; Beller, M.; Jiao, H. Structures and Energies of $[Co(CO)_n]^m$ ($m = 0, 1+, 1-$) and $HCo(CO)_n$: Density functional Studies. *J. Phys. Chem. A* **2002,** *106,* 12161.
29. Russell, D. H. *Gas Phase Inorganic Chemistry*; Plenum, New York: 1989.
30. Freiser, B. S. *Organometallic Ion Chemistry*; Kluwer: Dordrecht, The Netherlands, 1996.
31. (a) Khan, F. A.; Clemmer, D. E.; Schultz, R. H.; Armentrout, P. B. Sequential Bond Energies of Chromium Carbonyls ($Cr(CO)_x^+$, $x = 1$–6). *J. Phys. Chem.* **1993,** *97,* 7978. (b) Sievers, M. R.; Armentrout, P. B. Collision-Induced Dissociation Studies of V(CO) + x, x = 1–7: Sequential Bond Energies and the Heat of Formation of $V(CO)_6$. *J. Phys. Chem.* **1995,** *99,* 8135. (c) Meyer, F.; Chen, Y. M.; Armentrout, P. B. Sequential Bond Energies of $Cu(CO)_x^+$ and $Ag(CO)_x^+$ (x = 1–4). *J. Am. Chem. Soc.* **1995,** *117,* 4071. (d) Goebel, S.; Haynes, C. L.; Khan, F. A.; Armentrout, P. B. Collision-Induced Dissociation Studies of $Co(CO)_x^+$, x = 1–5: Sequential Bond Energies and Heats of Formation of $Co(CO)_4$. *J. Am. Chem. Soc.* **1995,** *117,* 6994. (e) Meyer, F.; Armentrout, P. B. Sequential Bond Energies of $Ti(CO)_x^+$, x = 1–7. *Mol. Phys.* **1996,** *88,* 187. (f) Zhang, X. G.; Armentrout, P. B. Sequential Bond Energies of $Pt(CO)_x^+$ (x = 1–4) Determined by Collision-Induced Dissociation. *Organometallics* **2001,** *20,* 4266.
32. (a) Grushow, A.; Ervin, K. M. Ligand and Metal Binding Energies in Platinum Carbonyl Cluster Anions: Collision-Induced Dissociation of Pt_m^- and $Pt_m(CO)_n^-$. *J. Chem. Phys.* **1997,** *106,* 9580. (b) Spasov, V. A.; Ervin, K. M. Binding Energies of Palladium Carbonyl Cluster Anions: Collision-Induced Dissociation of $Pd_3(CO)_n^-$ ($n = 0$–6). *J. Chem. Phys.* **1998,** *109,* 5344.

33. Le Caër, S.; Heninger, M.; Maitre, P.; Mestdagh, H. Accurate Measurement of the Relative Bond Energies of CO and H_2O ligands in Fe+ mono- and bis-ligated complexes. *Rapid Commun. Mass Spectrom.* **2003,** *17,* 351.

34. Schwartz, H. Relativistic Effects in Gas-Phase Ion Chemistry: An Experimentalist's View. *Angew. Chem. Int. Ed.* **2003,** *42,* 4442.

35. (a) Zhou, M.; Andrews, L. Infrared Spectra of $RhCO^+$, RhCO, and $RhCO^-$ in Solid Neon: A Scale for Charge Support in Catalyst Systems. *J. Am. Chem. Soc.* **1999,** *121,* 9171. (b) Zhou, M.; Andrews, L. Infrared Spectra and Density Functional Calculations of $CuCO_n^+$ ($n = 1–4$), $CuCO_n$ ($n = 1–3$), and $CuCO_n^-$ ($n = 1–3$), in Solid Neon. *J. Chem. Phys.* **1999,** *111,* 4548. (c) Zhou, M.; Andrews, L. Infrared Spectra and Density Functional Calculations of $RuCO^+$, $OsCO^+$, $Ru(CO)_x$, $Os(CO)_x$, $Ru(CO)_x^-$, and $Os(CO)_x^-$ ($x = 1–4$) in Solid Neon. *J. Phys. Chem. A* **1999,** *103,* 6956. (d) Zhou, M.; Andrews, L. Reactions of Laser-Ablated Iron Atoms and Cations with Carbon Monoxide: Infrared Spectra of $FeCO^+$, $Fe(CO)_2^+$, $Fe(CO)_x$, and $Fe(CO)_x^-$ ($x = 1–4$) in Solid Neon. *J. Chem. Phys.* **1999,** *110,* 10370. (e) Zhou, M.; Andrews, L. Matrix Infrared Spectra and Density Functional Calculations of ScCO, $ScCO^-$, and $ScCO^+$. *J. Phys. Chem. A* **1999,** *103,* 2964. (f) Zhou, M.; Andrews, L. Infrared Spectra and Density Functional Calculations for OMCO, and $OM-(\eta^2-CO^-)$, $OMCO^+$ and $OMOC^+$ (M = V, Ti) in Solid Argon. *J. Phys. Chem. A* **1999,** *103,* 5259. (g) Zhou, M.; Andrews, L. Reactions of Laser Ablated Co, Rh, and Ir with CO: Infrared Spectra and Density Functional Calculations of the Metal Carbonyl Molecules, Cations, and Anions in Solid Neon. *J. Phys. Chem. A* **1999,** *103,* 7773. (h) Liang, B.; Andrews, L. Reactions of Laser-Ablated Ag and Au Atoms with Carbon Monoxide: Matrix Infrared Spectra and Density Functional Calculations on $Au(CO)_n$ ($n = 2,3$), $Au(CO)_n^-$ ($n = 1,2$), and $M(CO)_n$ ($n = 1–4$), (M = Ag, Au). *J. Phys. Chem. A* **2000,** *104,* 9156. (i) Liang, B.; Zhou, M.; Andrews, L. Reactions of Laser-Ablated Ni, Pd, and Pt Atoms with Carbon monoxide: Matrix Infrared Spectra and Density Functional Calculations on $M(CO)_n$ ($n = 1–4$), $M(CO)_n^-$ ($n = 1–3$), and $M(CO)_n^+$ ($n = 1–2$), (M = Ni, Pd, Pt). *J. Phys. Chem. A* **2000,** *104,* 3905. (j) Andrews, L.; Zhou, M.; Wang, X.; Bauschlicher, C. W. Matrix Infrared Spectra and DFT Calculations of Manganese and Rhenium Carbonyl Neutral and Anion Complexes. *J. Phys. Chem. A* **2000,** *104,*8887.

36. Fielicke, A.; von Helden, G.; Meijer, G.; Pedersen, D. B.; Simard, B.; Rayner, D. M. Size and Charge Effects on Binding of CO to Small Isolated Rhodium Clusters. *J. Phys. Chem. B* **2004,** *108,* 14591.

37. Moore, D. T.; Oomens, J.; Eyler, J. R.; Meijer, G.; von Helden, G.; Ridge, D. P. Gas-Phase IR Spectroscopy of Anionic Iron Carbonyl Clusters. *J. Am. Chem. Soc.* **2004,** *126,* 14726.

38. (a) Fielicke, A.; von Helden, G.; Meijer, G.; Simard, B.; Rayner, D. M. Gold Cluster Carbonyls: Vibrational Spectroscopy of the Anions and the Effects of Cluster Size, Charge, and Coverage on the CO Stretching Frequency. *J. Phys. Chem. B* **2005,** *109,* 23935. (b) Fielicke, A.; von Helden, G.; Meijer, G.; Pedersen, D. B.; Simard, B.; Rayner, D. M. Gold Cluster Carbonyls: Saturated Adsorption of CO on Gold Cluster Cations, Vibrational Spectroscopy, and Implications for Their Structures. *J. Am. Chem. Soc.* **2005,** *127,* 8416.

39. Fielicke, A.; von Helden, G.; Meijer, G.; Pedersen, D. B.; Simard, B.; Rayner, D. M. Size and Charge Effects on the Binding of CO to Late Transition Metal Clusters. *J. Chem. Phys.* **2006,** *124,* 194305.

40. Duncan, M. A. Infrared Spectroscopy to Probe Structure and Dynamics in Metal Ion–Molecule complexes. *Intl. Rev. Phys. Chem.* **2003,** *22,* 407.

41. Walker, N. R.; Walters, R. S.; Duncan, M. A. Frontiers in the Infrared Spectroscopy of Gas Phase Metal Ion Complexes. *New J. Chem.* **2005,** *29,* 1495.

42. Velasquez, J. III; Njegic, B.; Gordon, M. S.; Duncan, M. A. IR Photodissociation Spectroscopy and Theory of $Au^+(CO)_n$ Complexes: Nonclassical Carbonyls in the Gas Phase. *J. Phys. Chem. A* **2008,** *112,* 1907.

43. Velasquez III, J.; Duncan, M. A. IR Photodissociation Spectroscopy of Gas Phase $Pt^+(CO)_n$ ($n = 4–6$). *Chem. Phys. Lett.* **2008,** *461,* 28.

44. Ricks, A. M.; Bakker, J. M.; Douberly, G. E.; Duncan, M. A. Infrared Spectroscopy and Structures of Cobalt Carbonyl Cations. *J. Phys. Chem. A* **2009,** *113,* 4701.

45. Ricks, A. M.; Reed, Z. D.; Duncan, M. A. Seven-Coordinate Homoleptic Metal Carbonyls in the Gas Phase. *J. Am. Chem. Soc.* **2009,** *131,* 9176–9177.

46. Seder, T. A.; Church, S. P.; Weitz, E. Gas-Phase Infrared Spectroscopy and Recombination Kinetics for Pentacarbonylmanganese Radical Generated Via Xenon Fluoride Laser Photolysis of Decacarbonyldimanganese. *J. Am. Chem. Soc.* **1986,** *108,* 1084.

47. Dearden, D. V.; Hayashibara, K.; Beauchamp, J. L.; Kirchner, N. J.; van Koppen, P. A. M.; Bowers, M. T. Fundamental Studies of the Energetics and Dynamics of Ligand Dissociation and Exchange Processes at Transition-Metal Centers in the Gas Phase: $Mn(CO)x^+$, x = 1–6. *J. Am. Chem. Soc.* **1989,** *111,* 2401.

48. Bauschlicher, C. W. Jr. On the Ground State of MnCŌ. *Chem. Phys. Lett.* **1996,** *249,* 244.

49. Becke, A. D. Three-Term Correlation Functional. *J. Chem. Phys.* **1993,** *98,* 5648.

50. Lee, C.; Yang, W.; Parr, R. G. Lee-Yang-Parr Correlation Functional. *Phys. Rev. B* **1998,** *98,* 5648.

51. Frisch, M. J.; Trucks, G. W.; Schlegel, H. B.; Scuseria, G. E.; Robb, M. A.; Cheeseman, J. R.; Montgomery, J. A., Jr.; Vreven, T.; Kudin, K. N.; Burant, J. C.; Millam, J. M.; Iyengar, S. S.; Tomasi, J.; Barone, V.; Mennucci, B.; Cossi, M.; Scalmani, G.; Rega, N.; Petersson, G. A.; Nakatsuji, H.; Hada, M.; Ehara, M.; Toyota, K.; Fukuda, R.; Hasegawa, J.; Ishida, M.; Nakajima, T.; Honda, Y.; Kitao, O.; Nakai, H.; Klene, M.; Li, X.; Knox, J. E.; Hratchian, H. P.; Cross, J. B.; Adamo, C.; Jaramillo, J.; Gomperts, R.; Stratmann, R. E.; Yazyev, O.; Austin, A. J.; Cammi, R.; Pomelli, C.; Ochterski, J. W.; Ayala, P. Y.; Morokuma, K.; Voth, G. A.; Salvador, P.; Dannenberg, J. J.; Zakrzewski, V. G.; Dapprich, S.; Daniels, A. D.; Strain, M. C.; Farkas, O.; Malick, D. K.; Rabuck, A. D.; Raghavachari, K.; Foresman, J. B.; Ortiz, J. V.; Cui, Q.; Baboul, A. G.; Clifford, S.; Cioslowski, J.; Stefanov, B. B.; Liu, G.; Liashenko, A.; Piskorz, P.; Komaromi, I.; Martin, R. L.; Fox, D. J.; Keith, T.; Al-Laham, M. A.; Peng, C. Y.; Nanayakkara, A.; Challacom, M.; Gill, P. M. W.; Johnson, B.; Chen, W.; Wong, M. W.; Gonzalez, C.; Pople, J. A. *Gaussian 03* (Rev. B.02); Gaussian, Inc.: Pittsburgh, PA, 2003.

52. Weigend, F.; Ahlrichs, R. Balanced Basis Sets of Split Valence, Triple Zeta Valence, and Quadruple Zeta Valence Quality for H to Rn: Design and Assessment of Accuracy. *Phys. Chem., Chem. Phys.* **2005,** *7,* 3297.

53. Schaefer, A.; Huber, R.; Ahlrichs, J. Fully Optimized Contracted Gaussian Basis Sets of Triple Zeta Valence Quality for Atoms Li to Kr. *J. Chem. Phys.* **1994,** *100,* 5829.

54. Partridge, H.; Bauschlicher, C. W.; Langhoff, S. R. Theoretical Study of Metal Ions Bound to Helium, Neon, and Argon. *J. Phys. Chem.* **1992,** *96,* 5350.

55. Ralchenko, Y.; Kramida, A. E.; Reader, J. NIST ASD Team (2008). *NIST Atomic Spectra Database* (ver. 3.1.5), [Online]. Available: *http://physics.nist.gov/asd3* [2009, November 19]. National Institute of Standards and Technology: Gaithersburg, MD.

56. Carnegie, P. D.; Bandyopadhyay, B.; Duncan, M. A. Infrared Spectroscopy of $Cr^+(H_2O)$ and $Cr^{2+}(H_2O)$: The Role of Charge in Cation Hydration. *J. Phys. Chem. A* **2008,** *112,* 6237.

57. Cramer, C. J.; Truhlar, D. G. Density Functional Theory for Transition Metals and Transition Metal Chemistry. *Phys. Chem., Chem. Phys.* **2009,** *11,* 10757.